Comprehensive transcriptomic profiling of liver cancer identifies that histone and PTEN are major regulators of SCU-induced antitumor activity

SANG EUN HA[1,2], ANJUGAM PARAMANANTHAM[1,3], HUN HWAN KIM[1], PRITAM BHAGWAN BHOSALE[1], MIN YEONG PARK[1], ABUYASEER ABUSALIYA[1], JEONG DOO HEO[2], WON SUP LEE[4] and GON SUP KIM[1]

[1]Research Institute of Life Science and College of Veterinary Medicine, Gyeongsang National University, Jinju, Gyeongsangnam-do 52828; [2]Gyeongnam Bio-Health Research Support Center, Gyeongnam Department of Environmental Toxicology and Chemistry, Korea Institute of Toxicology, Jinju, Gyeongsangnam-do 52834, Republic of Korea; [3]Department of Pathology and Anatomical Sciences, University of Missouri School of Medicine, Columbia, MO 65201, USA; [4]Department of Internal Medicine, Institute of Health Sciences and Gyeongsang National University Hospital, Gyeongsang National University College of Medicine, Jinju, Gyeongsangnam-do 52727, Republic of Korea

Received December 15, 2022; Accepted November 16, 2023

DOI: 10.3892/ol.2024.14227

Abstract. Worldwide, liver cancer is the most frequent fatal malignancy. Liver cancer prognosis is poor because patients frequently receive advanced-stage diagnoses. The current study aimed to establish the potential pharmacological targets and the biological networks of scutellarein (SCU) in liver cancer, a natural product known to have low toxicity and side effects. To identify the differentially expressed genes between SCU-treated and SCU-untreated HepG2 cells, RNA sequencing (RNA-seq) was carried out. A total of 463 genes were revealed to have differential expression, of which 288 were upregulated and 175 were downregulated in the group that had received SCU treatment compared with a control group. Gene Ontology (GO) enrichment analysis of associated biological process terms revealed they were mostly involved in the regulation of protein heterodimerization activity and nucleosomes. Interaction of protein-protein network analysis using Search Tool for the Retrieval of Interacting Genes/Proteins resulted in two crucial interacting hub targets; namely, histone H1-4 and protein tyrosine phosphatase receptor type C. Additionally, the crucial targets were validated using western blotting. Overall, the present study demonstrated that the use of RNA-seq data, with bioinformatics tools, can provide a valuable resource to identify the pharmacological targets that could have important biological roles in liver cancer.

Correspondence to: Professor Gon Sup Kim, Research Institute of Life Science and College of Veterinary Medicine, Gyeongsang National University, Gazwa Campus, 501 Jinju-daero, Jinju, Gyeongsangnam-do 52828, Republic of Korea
E-mail: gonskim@gnu.ac.kr

Key words: RNA-sequencing, differentially expressed genes, Gene Ontology, histone, PTEN, liver cancer, HepG2

Introduction

Liver cancer is still a primary global health concern, and its incidence rate is rising worldwide (1). According to the GLOBOCAN report from 2018, more than 1 million people will be diagnosed with liver cancer by 2025. The most prevalent form of liver cancer, known as human hepatocellular carcinoma (HCC), makes up around 90% of all cases that are detected (2). Because of the difficulty in getting an early diagnosis and the limited number of therapy options, the majority of patients with advanced-stage HCC have poor treatment outcomes (3). In recent years, novel treatment options for HCC have developed. Especially, many studies have investigated the synergistic effects and enhanced antitumor activity of combining locoregional and systemic therapies, based on strong biological rationale (4-7). Therefore, the creation of novel biomarkers and the creation of gene expression profiles are essential for improving early detection and precise prognosis as well as for offering a chance to better match the most efficient medications with the molecular characteristics of each patient (8).

A biomarker is defined as any substance, structure, or function that can be detected in the body, which influences or predicts the incidence of outcome or disease (9). This can be used to track early cancer detection, assess the prognosis, or gauge the effectiveness of therapy. The ideal biomarker is readily accessible, consistently measurable, cost-effective, and extremely accurate (10). In cancer, several recent advances have led to the diffusion of potential biomarkers, from genetic materials (e.g., DNA, epigenetic changes, cell-free DNA, RNA, mRNA), serum proteins, and circulating metabolites (11,12). Although there are several identified biomarkers

are available like glypican 3 (GPC3), Golgi protein-73 (GP73), descarboxypro-thrombin (DCP), glutamic pyruvic transaminase (GPT), gamma-glutamyl carboxylase (GGCX), and osteopontin (OPN) as complementary biomarkers for liver cancer diagnosis (13-16), the early and specific diagnosis of liver cancer remains challenging. Thus, it is crucial to identify more biomarkers concerning liver cancer for better treatment and prognosis.

The molecular mechanism of liver cancer is now better-understood thanks to the quick development of molecular biology tools like high throughput sequencing, microarrays, and different omics approaches. Epigenetics in particular has a well-established function and is just as important as genetics (17). Recent advances in the knowledge of the molecular biomarkers involved in the onset and progression of liver cancer as well as in the comprehensive mapping of the disease's key mechanisms have been made possible by the use of integrated multi-omics studies (18-20).

Transcriptomic analysis is a method that uses bioinformatics tools to examine changed target genes and comprehend the mechanism of action of a medicine after screening with an *in vitro* model (21). To better understand factors like particular pathways altered by a candidate meditation, differential gene expression under drug-treated disease conditions can be helpful (22). Additionally, gene expression information gleaned from transcriptome data can result in the discovery of new key genes connected to a pathway (23). Target identification with the use of natural products can accelerate patient-specific treatment methods.

New therapeutic alternatives are required for liver cancer patients. Using natural chemicals or nanotechnology could offer improved therapy with less toxicity and fewer side effects for patients, potentially leading to better prognoses (24). Scutellarein (SCU), a flavone present in the perennial herb *Scutellaria baicalensis*, is the aglycone of scutellarin with a free hydroxyl in 7 positions and has a higher bioavailability than scutellarin (25). Numerous research has shown that SCU may reduce the viability of human lung cancer cells and fibrosarcoma cells (26,27). It also depicted an anti-tumor effect in human colon cancer (28,29). In addition, our previous study showed that SCU inhibited cell proliferation and metastasis by upregulating PTEN in human hepatocellular carcinoma (30). First discovered as a tumor suppressor, PTEN (phosphatase and tensin homolog deleted on chromosome 10) is a highly targeted protein in a number of human illnesses (31,32). PTEN activity and expression appear to be regulated by a variety of intricate processes, which is consistent with these perspectives. Among these mechanisms, epigenetic silencing by hypermethylation of its promoter (33) or histone deacetylase activity (34) strongly affects PTEN expression. Even so, the mechanism of PTEN regulation remains elusive.

Histone modifications have long been assumed that they have a practical impact on the control of transcription (35). Linker histone H1 (Histone H1) is a chromatin structural component that aids in the structuring and stability of higher-order condensed chromatin structures (36). The higher expression of histone H1 shows that the SCU induces anti-tumor activity through histone H1 (37). PTEN physically binds with histone H1 to maintain a condensed chromatin structure, which is reflected by histone H1 chromatin occupancy and hypoacetylation of histone H4, resulting in suppression of overall gene activity (38). Knockdown of H1 in HCC1954 cells promoted an increase in renewable cancer stem cells (37).

Overall, the main objective of this study was to use a transcriptomic approach to find potential targets of SCU for treating liver cancer. Additionally, the study aimed to gain a deeper understanding of the connection between crucial targets that regulate PTEN, which has previously been identified as an anti-tumor agent for SCU (30).

Materials and methods

Cell culture. Human liver cancer HepG2 cell line was obtained from the Korean Cell Line Bank (Seoul, Korea). HepG2 cells were cultured in Dulbecco's modified Eagle's medium (DMEM) (Gibco; Thermo Fisher Scientific, Inc.) containing 10% fetal bovine serum (FBS) (Gibco; Thermo Fisher Scientific, Inc.), and 100 U/ml penicillin/100 μg/ml streptomycin (P/S) (Gibco; Thermo Fisher Scientific, Inc.) at 37˚C of 5% CO_2. Scutellarein (SCU) was purchased from Chengdu Biopurify Phytochemicals Ltd. (Chengdu, Sichuan, China).

Isolation of RNA for sequencing. HepG2 cells were seeded into 6-well plates at $1.5x10^5$ cells per well and treated with 100 μM of SCU for 48 h at 37˚C of 5% CO_2. After incubation, total RNAs were extracted using TRIzol (Ambion, Thermo Scientific, Rockford, IL, USA). The concentration of RNA was determined using a spectrophotometer (BioTek, Winooski, VT, USA). Isolated total RNA was then subjected to sequencing to obtain expression data.

Library preparation and sequencing. The mRNA sequencing was prepared by Theragenbio (Seongnam-si, Gyeonggi-do) using the following protocol (Table I). The libraries were prepared for 151bp paired-end sequencing using TruSeq stranded mRNA Sample Preparation Kit (Illumina, CA, USA). Utilizing oligo (dT) magnetic beads, mRNA molecules were specifically isolated and fragmented from 1 μg of total RNA. The fragmented mRNAs were synthesized as single-stranded cDNAs through random hexamer priming. Double-stranded cDNA was created by using this as a template for second-strand synthesis. After the sequential process of end repair, A-tailing, and adapter ligation, cDNA libraries were amplified with PCR (Polymerase Chain Reaction). The quality of these cDNA libraries was evaluated with the Agilent 2100 BioAnalyzer (Agilent, CA, USA). According to the manufacturer's library quantification methodology, they were measured using the KAPA library quantification kit (Kapa Biosystems, MA, USA). Following cluster amplification of denatured templates, sequencing was progressed as paired-end (2x151 bp) using Illumina NovaSeq6000 (Illumina, CA, USA).

Transcriptome data analysis

Filtering. The adapter sequences and ends of the reads less than Phred quality score 20 were trimmed and simultaneously the reads shorter than 50 bp were removed by using cutadapt v.2.8 (39).

Sequence alignment. Using the aligner STAR v.2.7.1a (40) and the 'quantMode TranscriptomeSAM' option for estimating

Table I. Sequencing statistics data.

No.	Name	Type	Reads, n (%)	Bases, n (%)	Bases, Gb	GC, n (%)	N, n (%)	Q30[a], n (%)
1	Control	Raw	45,235,978 (100.0%)	6,830,632,678 (100.0%)	6.83	3,408,682,904 (49.9%)	13,280 (0.0%)	6,416,713,568 (93.94%)
1	Control	Clean	44,943,094 (99.35%)	6,622,233,019 (96.95%)	6.62	3,292,325,453 (49.72%)	12,364 (0.0%)	6,246,152,632 (94.32%)
2	Test	Raw	41,769,186 (100.0%)	6,307,147,086 (100.0%)	6.31	3,307,569,595 (52.44%)	12,607 (0.0%)	5,872,870,702 (93.11%)
2	Test	Clean	41,372,112 (99.05%)	6,061,914,152 (96.11%)	6.06	3,173,001,276 (52.34%)	11,591 (0.0%)	5,674,328,197 (93.61%)

[a]Q30: Number of over Q30 bases (Q30: 99.9% Base Call Accuracy) (Q30/Bases x100).

transcriptome expression level, filtered reads were mapped to the reference genome associated with the species using ENCODE standard parameters (see to 'Alignment' of 'Help' section of the HTML report).

Gene expression estimation. By using the 'strandedness' option in RSEM v.1.3.1 (41) and taking into account the reads' direction in relation to the library technique, gene expression was estimated. The 'estimate-rspd' option was used to increase measurement accuracy. The default settings were used for all other options. FPKM (Fragments Per Kilobase Million) and TPM (Transcripts Per Kilobase Million) values were generated to standardize sequencing depth among samples.

Differentially expressed genes (DEG) analysis. The R package TCC v.1.26.0 was used to identify DEG based on the projected read counts from the preceding stage (42). TCC program compares tag count data using effective normalizing techniques. With the use of the iterative DESeq2 (43)/edgeR (44) approach, normalization factors were computed. Using the p.adjust function of the R package with the default parameter settings, the *q*-value was determined based on the P-value. Based on the *q*-value criterion of less than 0.05 for correcting mistakes brought on by multiple testing, the DEG were found.

Drug and disease association analyses. To predict drug and disease associations for candidate genes, our analysis was carried out in a functional database that was suggested (i.e., Drug Bank) by WEB-based GEne SeT AnaLysis (WebGestalt). Drug Bank and drug were chosen as the functional database and enrichment category, respectively, to predict the most important drugs for our target genes. The gene count was set at ≥ 5, and a P-value with a false discovery rate (FDR) adjusted of less than 0.05 was considered statistically significant. The WebGestalt derives significance results by clustering sets of genes using the Jaccard index as a criterion of similarity, prioritizing sets with significant P-value, and automatically identifying a 'model' or representative for each cluster (45).

miRNA-target enrichment analysis. Mienturnet (MicroRNA ENrichment TURned NETwork) is used to predict the miRNA target related to differentially regulated genes. 463 DEG was taken for prediction (both up and down-regulated). Out of 665 entries, we chose the top 10 entries based on the number of interactions.

Gene ontology (GO) analysis. GO database provides a set of hierarchical controlled vocabulary classified into 3 categories: Biological Process (BP), Cellular Component (CC), and Molecular Function (MF). For functional characterization of the DEG, a GO-based trend test was carried out using the R package called GOseq (46) through the Wallenius non-central hypergeometric distribution. Selected genes of P-value <0.05 following the test were regarded as statistically significant.

Molecular docking analysis. Molecular docking of Erlotinib and PTEN were performed using PyMol (The PyMOL Molecular Graphics System, Version 1.2r3pre, Schrödinger, LLC.) and USCF (47) chimera with the default parameters. Molecular docking of histone H1 and PTEN were performed using HDOCK server (http://hdock.phys.hust.edu.cn/) with the default parameters. Analysis for molecular interaction between histone H1 and PTEN was conducted through Discovery Studio 2018 (BIOVIA, San Diego, CA, USA).

STRING network analysis and pathway enrichment on the identifiable targets. The protein-protein interaction for up-regulated and down-regulated genes was performed using an online tool, Search Tool for the Retrieval of Interacting Genes/Proteins (STRING) (Accessed on 24, Jun 2021). Up-regulated gene interaction showed about 61 nodes, whereas the expected number of nodes was 57 (P-value; $1x10^{16}$). Down-regulated gene interaction showed about 26 nodes, whereas the expected number of nodes was 2 (P-value; $7.47x10^{11}$). Thus, the interaction was more significant than expected. In up-regulated genes, the significant pathways enriched were chosen based on KEGG, Wiki, and Reactome pathway analyses.

Western blot analysis. HepG2 cells were treated with indicated concentrations of SCU (0, 25, and 100) μM and lysed using radioimmunoprecipitation assay (RIPA) buffer (iNtRON Biotechnology, Seoul, Korea) containing phosphatase and protease inhibitor cocktail (Thermo Scientific, Rockford, IL, USA). Protein quantification were determined using a Pierce™ BCA assay (Thermo Fisher Scientific, Rockford, IL, USA). An equal quantity of protein (10 μg) from each sample

Table II. Differentially expressed genes.

No.	Controls	Cases	Sum	Genes	
				Up (controls < cases)	Down (controls > cases)
1	Control	Test	463	288	175

The analysis revealed total of 463 differentially expressed genes, 288 upregulated and 175 downregulated. The fold change criteria was set as ≥1.0.

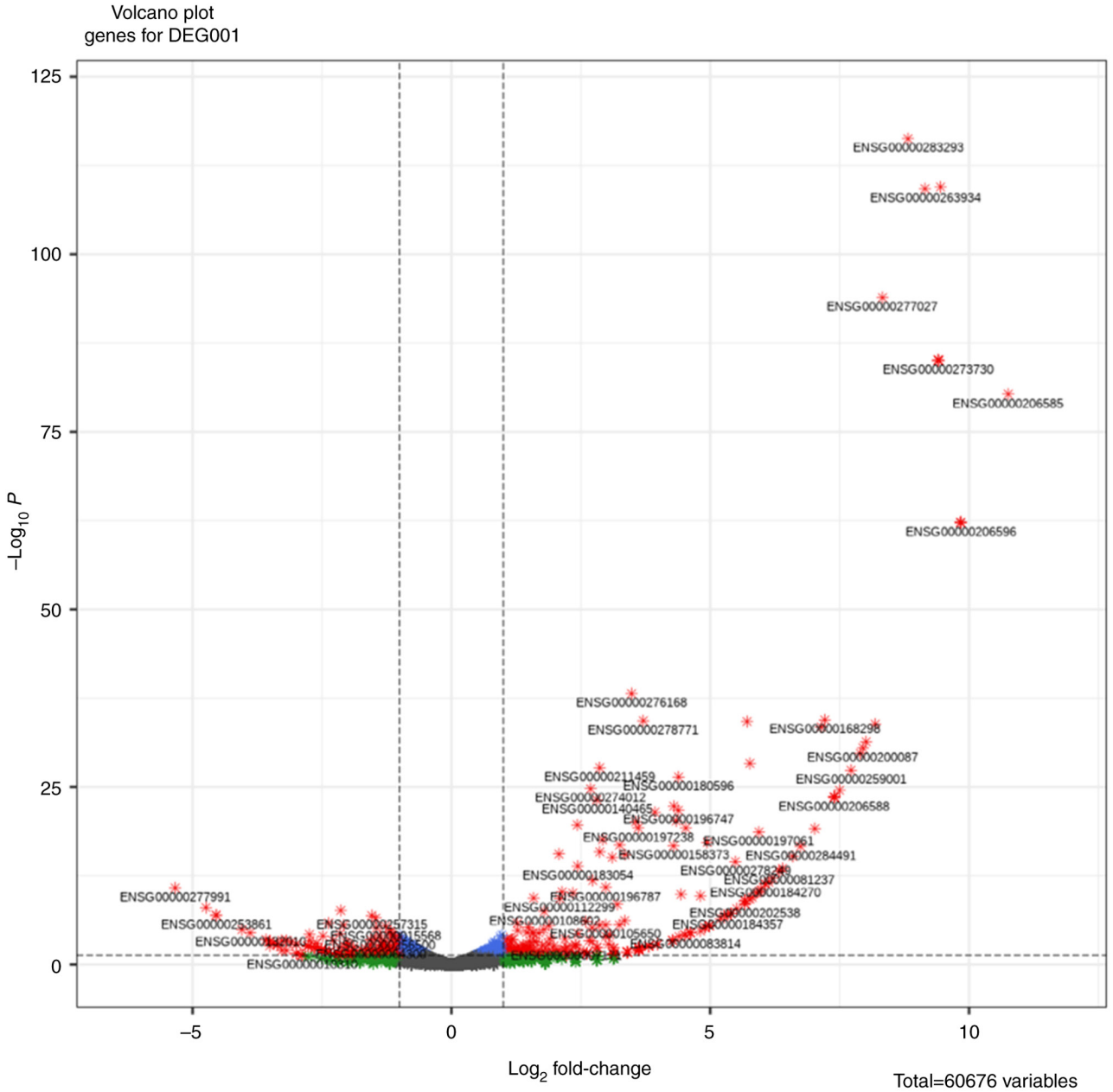

Figure 1. Volcano plot of differentially expressed genes. A total of 60,676 variables were considered for the plot. The fold-change was plotted based on -log10 P-value.

was electrophoresed on (8-15)% SDS-polyacrylamide gels and transferred to a polyvinylidene difluoride (PVDF) membrane (ATTO Co., Ltd., Tokyo, Japan). Membranes were blocked with 5% (bovine serum albumin (BSA) in Tris-buffered saline containing 1% Tween 20 (TBS-T, pH 7.4) at room temperature for 1 h, and incubated overnight at 4˚C with primary antibodies. The membranes were washed with TBS-T buffer for every 15 min in five times at room temperature, further

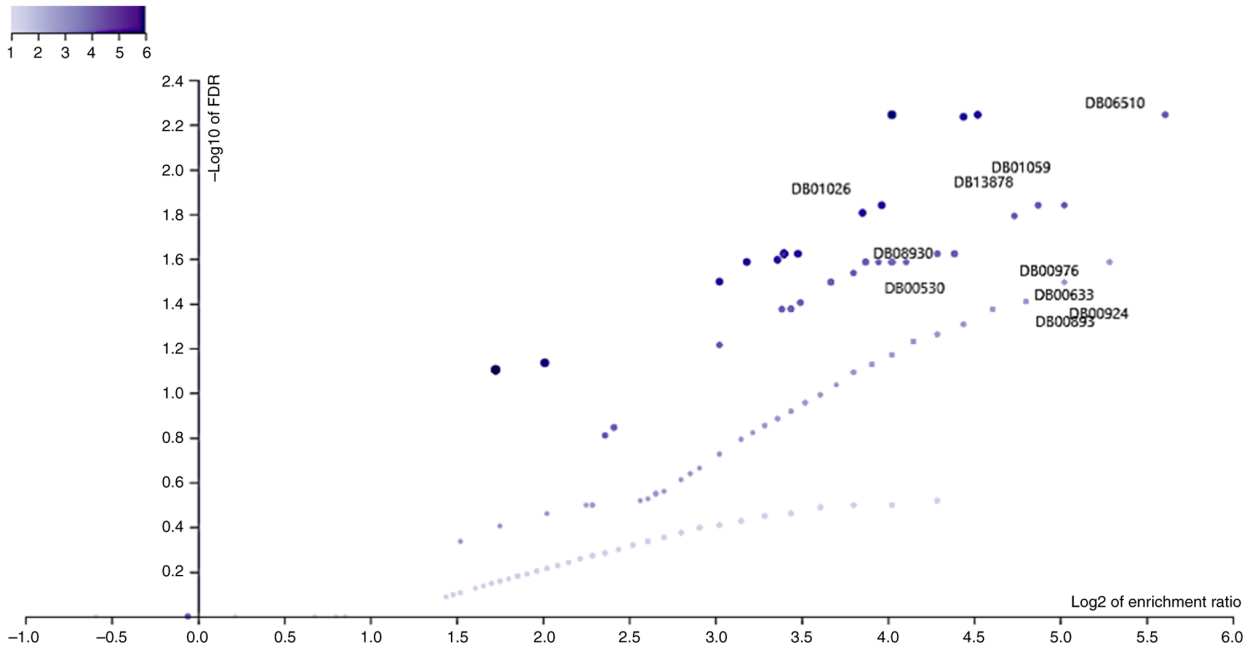

Figure 2. Scatter plot of drug and disease association analyses. The first 10 enriched drugs were presented in the plot. The entries were color-coded based on their FDR value.

they were incubated with 1:5,000 dilution of HRP-conjugated secondary antibody for 2-3 h at room temperature. The obtained proteins were detected by an electrochemiluminescence (ECL) detection system (Bio-Rad Laboratory, Hercules, CA, USA), and analyzed using the Image Lab 4.1 (Bio-Rad) program. The densitometry readings of the protein bands were normalized by comparison with the expression of β-actin as control, using the ImageJ software program (U.S. National Institutes of Health, Bethesda, MD, USA). Antibodies of histone H1-4 (Cat. no. 41328S), PTPRC (Cat. no. 72787S), and β-actin (Cat. no. 4970S) were purchased from Cell Signaling Technology (Danvers, MA, USA). Horseradish peroxidase (HRP)-conjugated secondary antibodies to anti-rabbit (cat. no. A120-101P) and anti-mouse (cat. no. A90-116P) were obtained from Bethyl Laboratories, Inc (Montgomery, USA).

Statistical analysis. Western blot experimental data were analyzed using GraphPad Prism version 8.0.2 (GraphPad Software). The findings were presented as the means ± standard deviation (SD) of triplicate samples. The unpaired Student's t-test was used to analyze the results, and a P-value of <0.05 was considered statistically significant.

Results

Identification of DEG. In our previous study on scutellarein (SCU) treatment in human liver cancer HepG2 cells, we revealed that SCU could inhibit cell proliferation and metastasis through PTEN activation in HepG2 cells (30). Herein, SCU-treated group were compared against the SCU-untreated group which unraveled about total of 463 DEG ($|\log_2 FC|>1.0$ and P-value <0.05), including 288 up-regulated and 175 down-regulated DEG (Table II). The DEG was represented as a volcano plot using an R-Bioconductor, which consists of a total of 60,676 variables (Fig. 1).

Therapeutic drug association analysis and molecular docking with PTEN. To identify the relationship between DEG and already available drugs we performed a drug-disease association analysis. After drug and disease association analyses (Fig. 2, Table III), we took the top 10 drugs which were significantly associated with DEG (FDR <0.05, gene count was set at ≥5). Among these drugs, the most effective cancer-specific drug is Erlotinib and which is a PTEN regulatory target drug (48). Furthermore, Erlotinib is associated with liver cancer, and it is used for the clinical treatment of liver cancer patients as a sole treatment or combination treatment with Sorafenib (49). To confirm the interaction of Erlotinib with PTEN, we performed drug and protein molecular docking (Fig. 3). UCSF Chimera software was used to validate the ligand-protein structures of these molecules. According to molecular docking studies, as shown in the image with the co-crystallized ligand, the two ligands occupied the active site. It was also discovered that many residues assisted in fitting the ligands into the binding pocket. The interacting amino acid residues involved in the bound complex of Erlotinib with PTEN were found to be PRO169, AGR172, ARG173, TYR176, TYR177, TYR180, PHE279, ILE280, PRO281, LEU318, THR319, LEU320, ASP324, and ASN323 (Table IV). The molecular dock scores suggest that the compound demonstrated PyMOL final intramolecular energy of -7.45 kcal/mol. In summary, SCU is associated with the drug Erlotinib, which is used as a clinical drug to treat PTEN-related diseases such as liver cancer. The development and use of peptides or inhibitors that target PTEN-related kinases, transcription factors, and cellular proteins could have a significant therapeutic benefit in the treatment of PTEN-related diseases (48). Therefore, we strongly suggest a strong relationship between DEG and PTEN.

miRNA-DEG target prediction. Target identification of miRNA concerning DEG was performed with the use of an

Table III. Results of drug and disease association analyses.

Gene set	Description	Size	Expect	Ratio	P-value	FDR
DB06510	Muraglitazar	6	0.061454	48.817	0.000019008	0.0056961
DB01059	Norfloxacin	9	0.092182	32.544	0.000078191	0.014458
DB13878	Pibrentasvir	10	0.10242	29.29	0.00011093	0.014458
DB01026	Ketoconazole	27	0.27654	14.464	0.00013337	0.015644
DB00530	Erlotinib	14	0.14339	20.921	0.00032728	0.023835
DB08930	Dolutegravir	14	0.14339	20.921	0.00032728	0.023835
DB00633	Dexmedetomidine	5	0.051212	39.053	0.00099517	0.025941
DB00893	Iron Dextran	5	0.051212	39.053	0.00099517	0.025941
DB00924	Cyclobenzaprine	5	0.051212	39.053	0.00099517	0.025941
DB00976	Telithromycin	5	0.051212	39.053	0.00099517	0.025941

A list of enriched drug with respect to differentially expressed gene set were depicted. The top 10 drugs were chosen based on their significance rate. FDR, false discovery rate.

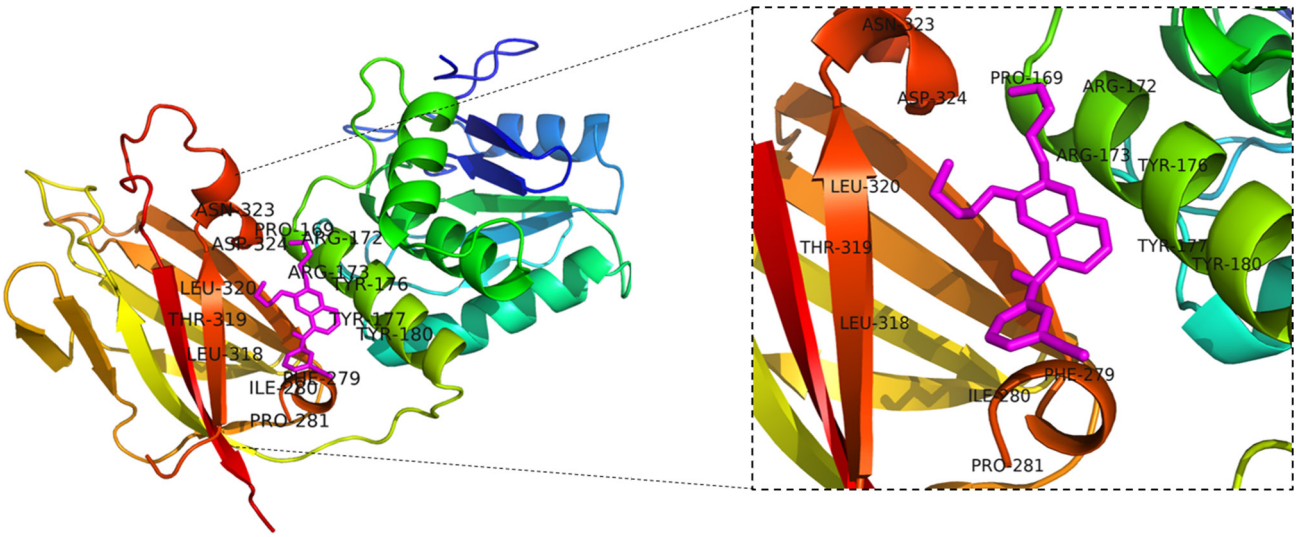

Figure 3. Molecular docking analysis of Erlotinib and PTEN. The 3D structure of protein PTEN bound efficiently with the compound Erlotinib were shown with their interacting amino acids.

online tool Mienturnet (MicroRNA ENrichment TURned NETwork). Mienturnet predicts the target miRNA based on statistical analysis, network-based visualization, and analysis. Around 665 putative target miRNA were predicted concerning 463 DEG. The top 10 miRNA targets were selected based on the number of interactions and plotted in a graph. miR-335-5p and miR-26b-5p showed a high number of target interactions which is about 34 and 14 (Fig. 4).

Functional and enrichment analysis. Functional enrichment analysis is a method for locating gene or protein classes that are disproportionately represented in a big collection of genes or proteins that may be associated with anti-tumor properties. When these hub genes were subjected to enrichment analysis to identify significant gene ontology (GO) terms, a list of up-regulated and down-regulated genes involved in nucleosomes, cellular content, and molecular function were shown in Fig. 5. The highly expressed function in each category is listed in Table V. Additionally, Linker histone H1 (Histone H1) was involved in all obtained enriched functional analyses.

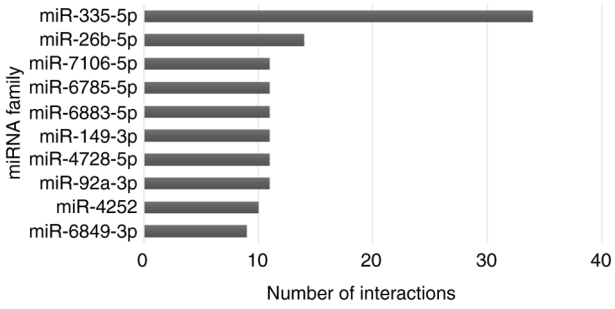

Figure 4. miR-target enrichment analysis. miR targets were identified using Mienturnet. Out of 665 obtained miR targets, the top 10 were plotted in a graph with respect to the number of interactions in differentially expressed genes. miR, microRNA.

Table IV. Molecular docking studies of selected target drug with PTEN and their binding energies.

Drug-protein	Interacting amino acid residues	Final intermolecular energy, kcal/mol	Final total energy, kcal/mol	Torsinal free energy, kcal/mol	Unbound system's energy, kcal/mol
Erlotinib	PRO169, AGR172, ARG173, TYR176, TYR177, TYR180, PHE279, ILE280, PRO281, LEU318, THR319, LEU320, ASP324, ASN323	-7.45	-1.33	+2.98	-1.33

The table shows the list of interacting amino acids and their binding energy.

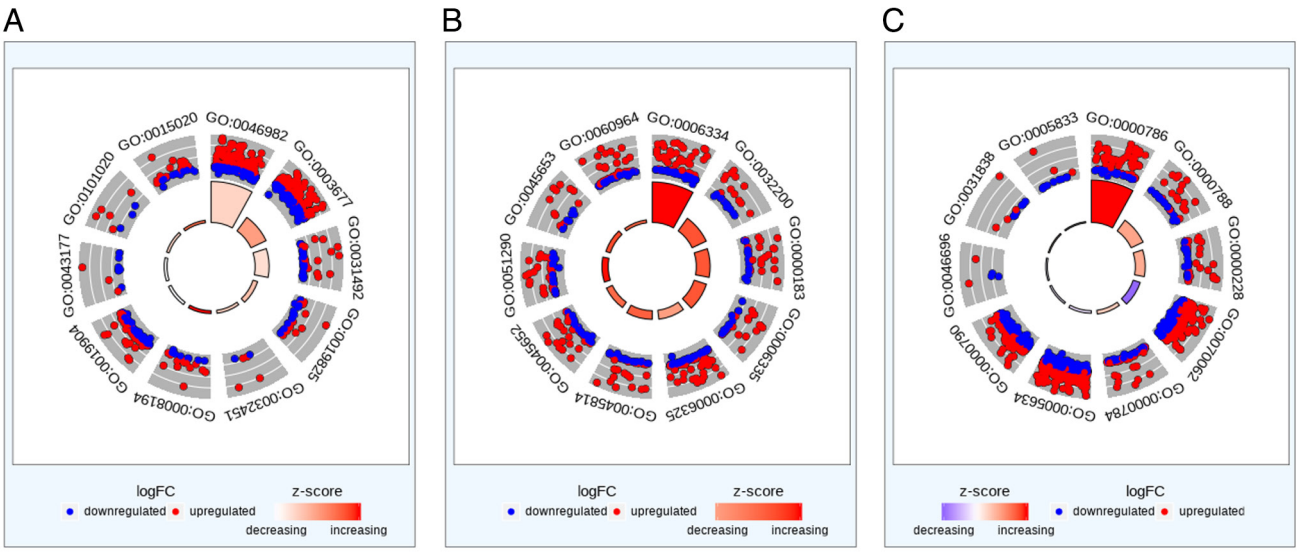

Figure 5. Circos plot representation of gene enrichment ontology analysis plotted in terms of (A) molecular function, (B) biological process and (C) cellular component of SCU against HCC. SCU, scutellarein; HCC, hepatocellular carcinoma; GO, Gene Ontology.

PPI network interaction and pathway enrichment analysis. Fig. 6A and B show the protein-protein interaction (PPI) network of up-regulated and down-regulated genes. The histone has a higher degree of the up-regulated PPI network, including 61 nodes and 293 edges. In contrast, the down-regulated PPI network, including 26 nodes and 17 edges, shows no significant relations. The figure summarizes the network of anticipated connections for a specific protein group. The edges represent the anticipated functional connections based on seven types of evidence: fusion evidence, neighborhood evidence, concurrence evidence, experimental evidence, text mining evidence, database evidence, and co-expression evidence. In addition, the pathway enrichment analysis of the potential targets were identified using different database (Table VI). Table VI lists the results of the screening. The KEGG database were found to be necroptosis, drug metabolism, pentose and glucuronate interconversions, porphyrin and chlorophyll metabolism, and phagosome pathway. Wiki database was found to be histone modifications, codeine and morphine metabolism, tamoxifen metabolism, and translation factors pathway. Reactome database shown to be HDACs deacetylate histones, DNA methylation, PRC2 methylates histones and DNA, Transcriptional regulation by small RNAs, deubiquitination, apoptosis induced DNA fragmentation, and caspase activation via death receptors in the presence of ligand pathway.

Crucial target molecular docking. The interactions among these three nodes and their first adjacent nodes were used to construct the sub-network (Fig. 7A-D). In our previous study, we have shown that SCU anti-tumor activity is regulated by PTEN (30), and transcriptomics analysis showed the role of histone is evident. To unravel the interaction between PTEN and histone H1, we performed molecular docking.

Validation of target protein expression using western blot assay. After examining the STRING analysis, the two crucial targets were validated by western analysis on SCU-treated HepG2 cells. These selected target proteins histone H1-4 (H1-4) and protein tyrosine phosphatase receptor type C (PTPRC) upon treatment with 100 μM of SCU in HepG2 cells. Fig. 8 shows that SCU up-regulated the expression of histone H1-4 (H1-4) and PTPRC respectively. These results further certify the role of SCU in regulating the expression of crucial targets in HepG2 cells.

Table V. List of enriched GO in terms of (A) molecular function, (B) biological process and (C) cellular component.

A, Molecular function

Gene ID	Term	Z-score
GO:0046982	Protein heterodimerization activity	0.751
GO:0003677	DNA binding	1.680
GO:0031492	Nucleosomal DNA binding	0.577
GO:0019825	Oxygen binding	1.091
GO:0032451	Demethylase activity	0.816
GO:0008194	UDP-glycosyltransferase activity	3.357
GO:0019904	Protein domain specific binding	-0.067
GO:0043177	Organic acid binding	0.000
GO:0101020	Estrogen 16-alpha-hydroxylase activity	0.707
GO:0015020	Glucuronosyltransferase activity	2.400

B, Biological process

Gene ID	Term	Z-score
GO:0006334	Nucleosome assembly	2.491
GO:0032200	Telomere organization	2.065
GO:0000183	Chromatin silencing at Rdna	2.043
GO:0006335	DNA replication-dependent nucleosome assembly	2.041
GO:0006325	Chromatin organization	1.237
GO:0045814	Negative regulation of gene expression, epigenetic	1.938
GO:0045652	Regulation of megakaryocyte differentiation	1.838
GO:0051290	Protein heterotetramerization	2.469
GO:0045653	Negative regulation of megakaryocyte differentiation	2.138
GO:0060964	Regulation of gene silencing by miRNA	1.886

C, Cellular component

Gene ID	Term	Z-score
GO:0000786	Nucleosome	5.501
GO:0000788	Nuclear nucleosome	2.558
GO:0000228	Nuclear chromosome	2.402
GO:0070062	Extracellular exosome	-3.607
GO:0000784	Nuclear chromosome, telomeric region	1.460
GO:0005634	Nucleus	-0.667
GO:0000790	Nuclear chromatin	-0.53
GO:0046696	Lipopolysaccharide receptor complex	-0.447
GO:0031838	Haptoglobin-hemoglobin complex	0.816
GO:0005833	Hemoglobin complex	0.000

GO, Gene Ontology.

Discussion

The development of RNA sequencing (RNA-seq) technology has increased the potential of RNA-based biomolecules for diagnostic, prognostic, and therapeutic applications in a variety of disorders, including cancer and many infectious diseases. (50). The complexity of cancer is made up of many different transcriptional programs that are widely linked with tumor cell populations. These transcriptional programs are also thought to be the main causes of therapy resistance, recurrence, and poor prognosis (51). Improved patient-specific treatment options were made possible by the use of RNA-seq analysis to identify gene expression and transcriptional changes in cancer patients (52).

Table VI. Pathway enrichment analysis of the predicted targets of scutellarein.

A, KEGG pathways

Pathway ID	Description	Strength	FDR
Hsa04217	Necroptosis	1.33	$4.86x10^{9}$
Hsa00982	Drug metabolism-cytochrome P450	1.3	0.0022
Hsa00040	Pentose and glucoronate interconversions	1.46	0.0058
Hsa00860	Porphyrin and chlorophyll metabolism	1.37	0.0097
Hsa04145	Phagosome	0.96	0.0285

B, Wiki pathways

Pathway ID	Description	Strength	FDR
WP2369	Histone modifications	1.34	0.0475
WP1604	Codeine and morphine metabolism	1.81	0.0076
WP691	Tamoxifen metabolism	1.66	0.0125
WP107	Translation factors	1.29	0.0480

C, Reactome Pathways

Pathway ID	Description	Strength	FDR
Hsa3214815	HDACs deacetylate histones	1.98	$1.85x10^{26}$
Hsa5334118	DNA methylation	2.15	$1.70x10^{24}$
Hsa212300	PRC2 methylates histones and DNA	2.06	$1.37x10^{23}$
Hsa5578749	Transcriptional regulation by small RNAs	1.8	$9.69x10^{21}$
Hsa5688426	Deubiquitination	1.34	$1.09x10^{18}$
Hsa140342	Apoptosis-induced DNA fragmentation	1.87	0.0003
Hsa109581	Apoptosis	0.97	0.0048
Hsa140534	Caspase activation via death receptors in the presence of ligand	1.6	0.0278

Hereby, we analyzed the anti-cancer regulatory genes including anti-tumor, proliferation, and metastasis of scutellarein (SCU) in HepG2 cells with the use of RNA-seq. We observed 60,676 variables of genes demonstrating differential expression compared with the SCU-untreated group and SCU-treated group. The analysis revealed a total of 463 significant differentially expressed genes (DEG), 288 up-regulated and 175 down-regulated.

Based on the DEG data, drug and disease association analyses were performed. The first 10 enriched drugs were sorted, and among those on the top list, it was confirmed through previous studies that Erlotinib was related to PTEN (48). The target of Erlotinib is the epidermal growth factor receptor (EGFR), and it has been found that there is a 'PTEN loss contributes to Erloninib resistance' effect. The reference provider name used for the current patient is OSI Pharmaceuticals US6900221 (53). In our previous study, we revealed that SCU is a potent PTEN activator (30). Therefore, these findings suggest that SCU may have a similar function to Erlotinib, thus consistent with our previous study.

The obtained DEG participates in various regulatory networks. We conducted a gene ontology (GO) analysis to determine their molecular function, biological process, and cellular component. The results showed that genes related to histone and linker histone were ranked high in all three terms. Protein heterodimerization activity is highly enriched in the molecular function that consists of 42 genes of DEG. Protein heterodimerization is a highly conserved process and any deregulation in this process might lead to several inflammatory diseases. Histones function within the nucleus to package and organize DNA (54). The great degree of conservation of histones H3 and H4 throughout eukaryotic evolution suggests that they are crucial for structural and functional functions (55,56). These histones exist in chromatin in a precise stoichiometry and wrap DNA to provide a crucial architectural framework for the nucleosome (57). Histone H4 interacts with H3 via their C-terminal histone fold domains to form heterodimers (55). Interestingly, nucleosome assembly is also highly enriched in a biological process that consists of 28 genes of DEG.

Furthermore, the nucleosome assembly's synonym is histone chaperone. When histones are deposited during nucleosome formation or when histones are disassembled, histone chaperones are involved (58). The nucleosome is

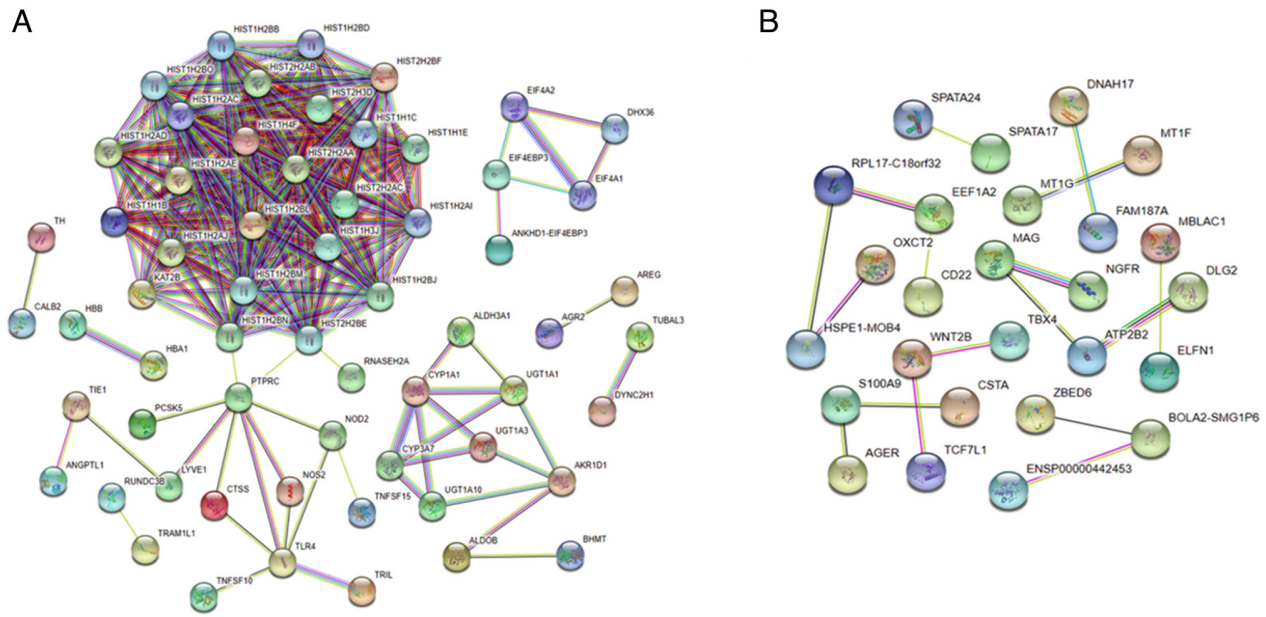

Figure 6. Protein-protein interaction analysis using Search Tool for the Retrieval of Interacting Genes/Proteins. The figure represents the interaction of (A) upregulated gene expression and (B) downregulated gene expression. The molecules were color-coded based on their expression pattern. The thickness of the line corresponds to the strength of the interaction between the proteins.

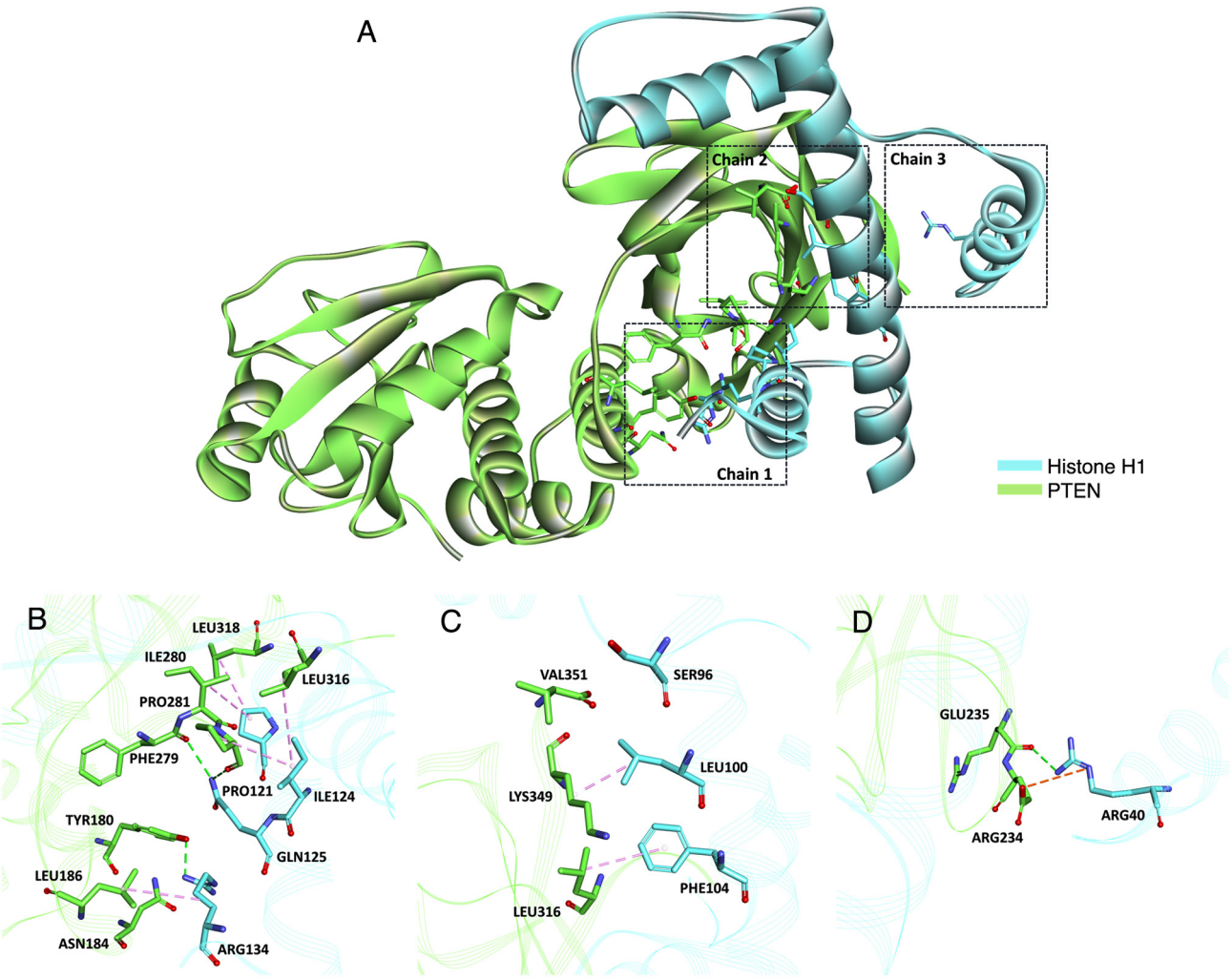

Figure 7. Molecular docking verification of association between the crucial targets histone H1 and PTEN. (A) 3D model of histone H1-PTEN complex. Histone H1 (cyan) and PTEN (lime) are shown in cartoon ribbon. Atomic interaction analysis between of PTEN and chain (B) 1, (C) 2 and (D) 3 on histone H1, respectively. Hydrogen bond, electrostatic and hydrophobic interactions are represented by the green, orange and magenta dashed lines, respectively.

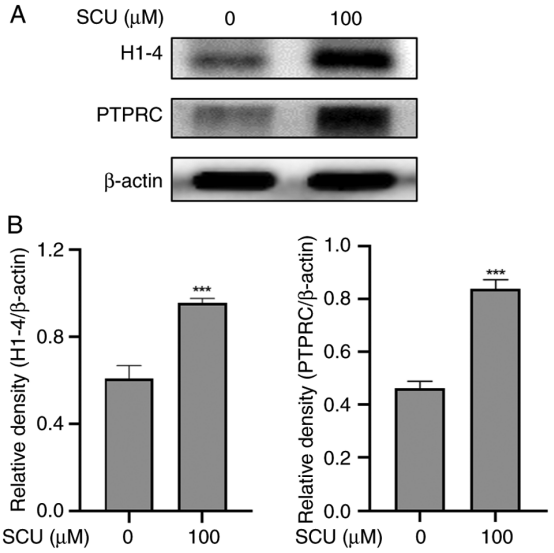

Figure 8. Western blotting validation of crucial targets of SCU against HCC. (A) Expression of crucial targets as histone H1-4 (H1-4) and PTPRC on SCU-treated HepG2 cells for 48 h. Graphical representations of protein expression were shown and the proteins were normalized with an internal control β-actin. (B) Results obtained from three independent experiments were expressed as mean ± standard deviation (SD) compared with the control group. ***P<0.001. PTPRC, protein tyrosine phosphatase receptor type C; SCU, scutellarein; HCC, hepatocellular carcinoma; H1-4, histone H1-4.

highly enriched in the cellular component that consists of 98 genes of DEG. miRNA prediction also showed the highly enriched miRNA-335-5p is related to histone (59). In addition, as a tumor suppressor in human hepatocellular carcinoma (HCC), miRNA-335-5p inhibited the growth, proliferation, and invasion of liver cancer cells (60). miRNA-26B-5P is associated with PTEN (61). Thus, it regulates the proliferation, angiogenesis, and apoptosis in liver cancer (62).

In summary, all the results obtained from our study indicate that they are associated with histone-related functions. Our previous study showed that SCU regulates the PTEN-PI3K pathway. Interestingly, RNA-seq analysis revealed a differential regulation of genes related to histones. This discovery intrigued us to investigate the relationship between PTEN and histones. Therefore, we hypothesized that SCU regulates cell proliferation by sequentially modulating the activity of histones and PTEN. Protein-protein interaction (PPI) analysis using Search Tool for the Retrieval of Interacting Genes/Proteins (STRING) confirmed that the histone-related groups were highly interconnected. Among the histone group, linker histone H1-4 (H1-4) which showed the highest fold change value was taken to analyze the different associations with PTEN. Many studies have shown that PTEN forms a complex with histone H1 to promote a condensed chromatin structure, the presence of histone H1 in chromatin, and hypoacetylation of histone H4 leads to suppression of overall gene activity (38,63). In addition, the molecular interaction of the histone H1 showed active binding sites in all three chains with PTEN in docking analysis. GO analysis of DEG showed many enriched genes associated with the nucleosomes, like histones, emphasizing the PTEN-Histone relation, which falls in line with our hypothesis. In a recent study, Chen et al. showed that interaction between PTEN and histone H1 decreased H4K16 acetylation (38). Thus, PTEN is responsible for maintaining genomic integrity and preventing tumor growth. Therefore, histone H1-4 (H1-4) has a crucial role in SCU-induced anti-tumor activity. Accordingly, the closely linked protein tyrosine phosphatase receptor type C (PTPRC) proteins, including histone H1-4 (H1-4), were selected as important targets. PTPRC correlates with colorectal cancer disease stage and outcome, according to research (64). To support the prior research, we performed protein expression analysis for specific genes. The protein expression level of these two crucial targets matched our transcriptomic results.

Taken together, the analysis results of DEG and GO data provide insight into anti-cancer treatment in SCU-treated HepG2 cells. In this present study, we found that SCU induces upregulation of histone H1, histone H1 forms a complex with PTEN and regulates the crucial target gene, PTPRC. Consistent with our previous study, the current results support that SCU inhibits the proliferation of HepG2 cells by its molecular action with the PTEN-PI3K pathway. Targeting the pathway can be an attractive strategy for cancer treatment, and SCU can be used as a target drug to inhibit PI3K/Akt signaling, a downstream pathway, by activating PTEN. It has been demonstrated that targeted therapy can be attributed to aberrant expression of signal transduction pathways such PTEN/PI3K/Akt (65). This study focuses in-depth on PTEN/PI3K/Akt-related gene changes as the cause of this pathway's dysregulated expression. The expression of this pathway can be controlled to enhance cancer treatment. Therefore, it suggests that SCU, a natural product known to have few side effects, can be considered as a potential treatment for liver cancer.

As a result of this study, further preclinical and clinical trials are needed to implement a treatment strategy, but it can be used to provide basic data for the development of new drugs derived from natural products and for mechanism research.

Acknowledgements

Not applicable.

Funding

This study was supported by the National Research Foundation of Korea funded by the Ministry of Science and ICT (grant nos. 2022R1A6A3A01086899 and RS-2023-00243376613 82).

Availability of data and materials

The datasets used and analyzed during the current study are available from the GEO database (accession no. GSE232800; https://www.ncbi.nlm.nih.gov/geo/query/acc.cgi?&acc=GSE232800). The other datasets used and/or analyzed during the current study are available from the corresponding author on reasonable request.

Author's contributions

SEH conceptualized the study. AP designed the methodology. SEH and AP performed the analysis of data, and wrote and prepared the original draft. SEH and AP confirmed the

authenticity of all the raw data. SEH wrote, reviewed, and edited the manuscript. HHK and PBB performed the interpretation of data and revised the final manuscript. MYP and AA performed some experiments and validation of data. JDH and WSL contributed to the study conception and design. GSK conceptualized and supervised the study. All authors read and approved the final version of the manuscript.

Ethics approval and consent to participate

Not applicable.

Patient consent for publication

Not applicable.

Competing interests

The authors declare that they have no competing interests.

References

1. Llovet JM, Zucman-Rossi J, Pikarsky E, Sangro B, Schwartz M, Sherman M and Gores G: Hepatocellular carcinoma. Nat Rev Dis Primers 2: 16018, 2016.
2. Di Bisceglie AM, Rustgi VK, Hoofnagle JH, Dusheiko GM and Lotze MT: NIH conference. Hepatocellular carcinoma. Ann Intern Med 108: 390-401, 1988.
3. Villanueva A and Llovet JM: Targeted therapies for hepatocellular carcinoma. Gastroenterology 140: 1410-1426, 2011.
4. Rizzo A, Ricci AD and Brandi G: Systemic adjuvant treatment in hepatocellular carcinoma: Tempted to do something rather than nothing. Future Oncol 16: 2587-2589, 2020.
5. Santoni M, Rizzo A, Mollica V, Matrana MR, Rosellini M, Faloppi L, Marchetti A, Battelli N and Massari F: The impact of gender on The efficacy of immune checkpoint inhibitors in cancer patients: The MOUSEION-01 study. Crit Rev Oncol Hematol 170: 103596, 2022.
6. Rizzo A, Ricci AD and Brandi G: Trans-arterial chemoembolization plus systemic treatments for hepatocellular carcinoma: An update. J Pers Med 12: 1788, 2022.
7. Rizzo A, Ricci AD and Brandi G: Atezolizumab in advanced hepatocellular carcinoma: Good things come to those who wait. Immunotherapy 13: 637-644, 2021.
8. Bazzichetto C, Conciatori F, Pallocca M, Falcone I, Fanciulli M, Cognetti F, Milella M and Ciuffreda L: PTEN as a Prognostic/Predictive biomarker in cancer: An unfulfilled promise? Cancers (Basel) 11: 435, 2019.
9. Sengupta S and Parikh ND: Biomarker development for hepatocellular carcinoma early detection: Current and future perspectives. Hepat Oncol 4: 111-122, 2017.
10. Ptolemy AS and Rifai N: What is a biomarker? Research investments and lack of clinical integration necessitate a review of biomarker terminology and validation schema. Scand J Clin Lab Invest 242: 6-14, 2010.
11. Tovar V, Cornella H, Moeini A, Vidal S, Hoshida Y, Sia D, Peix J, Cabellos L, Alsinet C, Torrecilla S, *et al*: Tumour initiating cells and IGF/FGF signalling contribute to sorafenib resistance in hepatocellular carcinoma. Gut 66: 530-540, 2017.
12. Sia D, Villanueva A, Friedman SL and Llovet JM: Liver cancer cell of origin, molecular class, and effects on patient prognosis. Gastroenterology 152: 745-761, 2017.
13. Jing JS, Ye W, Jiang YK, Ma J, Zhu MQ, Ma JM, Zhou H, Yu LQ, Yang YF and Wang SC: The value of GPC3 and GP73 in clinical diagnosis of hepatocellular carcinoma. Clin Lab 63: 1903-1909, 2017.
14. Wongjarupong N, Negron-Ocasio GM, Chaiteerakij R, Addissie BD, Mohamed EA, Mara KC, Harmsen WS, Theobald JP, Peters BE, Balsanek JG, *et al*: Model combining pre-transplant tumor biomarkers and tumor size shows more utility in predicting hepatocellular carcinoma recurrence and survival than the BALAD models. World J Gastroenterol 24: 1321-1331, 2018.
15. Ono K, Kokubu S, Hidaka H, Watanabe M, Nakazawa T and Saigenji K: Risk factors of delay in restoration of hepatic reserve capacity and local recurrence after radiofrequency ablation therapy for hepatocellular carcinoma (HCC). Hepatol Res 31: 172-177, 2005.
16. Zhu M, Zheng J, Wu F, Kang B, Liang J, Heskia F, Zhang X and Shan Y: OPN is a promising serological biomarker for hepatocellular carcinoma diagnosis. J Med Virol 92: 3596-3603, 2020.
17. Luo XY, Wu KM and He XX: Advances in drug development for hepatocellular carcinoma: Clinical trials and potential therapeutic targets. J Exp Clin Cancer Res 40: 172, 2021.
18. Cancer Genome Atlas Research Network. Electronic address: wheeler@bcm.edu; Cancer Genome Atlas Research Network: Comprehensive and integrative genomic characterization of hepatocellular carcinoma. Cell 169: 1327-1341 e1323, 2017.
19. Schulze K, Imbeaud S, Letouze E, Alexandrov LB, Calderaro J, Rebouissou S, Couchy G, Meiller C, Shinde J, Soysouvanh F, *et al*: Exome sequencing of hepatocellular carcinomas identifies new mutational signatures and potential therapeutic targets. Nat Genet 47: 505-511, 2015.
20. Hardy T and Mann DA: Epigenetics in liver disease: From biology to therapeutics. Gut 65: 1895-1905, 2016.
21. Luo J, Dai X, Hu H, Chen J, Zhao L, Yang C, Sun J, Zhang L, Wang Q, Xu S, *et al*: Fluzoparib increases radiation sensitivity of non-small cell lung cancer (NSCLC) cells without BRCA1/2 mutation, a novel PARP1 inhibitor undergoing clinical trials. J Cancer Res Clin Oncol 146: 721-737, 2020.
22. Wang D, Zhao L, Wang D, Liu J, Yu X, Wei Y and Ouyang Z: Transcriptome analysis and identification of key genes involved in 1-deoxynojirimycin biosynthesis of mulberry (Morus alba L.). PeerJ 6: e5443, 2018.
23. Zhang Y, Kang Z, Lv D, Zhang X, Liao Y, Li Y, Liu R, Li P, Tong M, Tian J, *et al*: Longitudinal whole-genome sequencing reveals the evolution of MPAL. Cancer Genet 240: 59-65, 2020.
24. Anwanwan D, Singh SK, Singh S, Saikam V and Singh R: Challenges in liver cancer and possible treatment approaches. Biochim Biophys Acta Rev Cancer 1873: 188314, 2020.
25. Shi X, Chen G, Liu X, Qiu Y, Yang S, Zhang Y, Fang X, Zhang C and Liu X: Scutellarein inhibits cancer cell metastasis *in vitro* and attenuates the development of fibrosarcoma *in vivo*. Int J Mol Med 35: 31-38, 2015.
26. Cheng CY, Hu CC, Yang HJ, Lee MC and Kao ES: Inhibitory effects of scutellarein on proliferation of human lung cancer A549 cells through ERK and NFkappaB mediated by the EGFR pathway. Chin J Physiol 57: 182-187, 2014.
27. Parajuli P, Joshee N, Rimando AM, Mittal S and Yadav AK: In vitro antitumor mechanisms of various Scutellaria extracts and constituent flavonoids. Planta Med 75: 41-48, 2009.
28. Guo F, Yang F and Zhu YH: Scutellarein from Scutellaria barbata induces apoptosis of human colon cancer HCT116 cells through the ROS-mediated mitochondria-dependent pathway. Nat Prod Res 33: 2372-2375, 2019.
29. Goh D, Lee YH and Ong ES: Inhibitory effects of a chemically standardized extract from Scutellaria barbata in human colon cancer cell lines, LoVo. J Agric Food Chem 53: 8197-8204, 2005.
30. Ha SE, Kim SM, Vetrivel P, Kim HH, Bhosale PB, Heo JD, Lee HJ and Kim GS: Inhibition of cell proliferation and metastasis by scutellarein regulating PI3K/Akt/NF-kappaB signaling through PTEN activation in hepatocellular carcinoma. Int J Mol Sci 22: 8841, 2021.
31. Wiencke JK, Zheng S, Jelluma N, Tihan T, Vandenberg S, Tamgüney T, Baumber R, Parsons R, Lamborn KR, Berger MS, *et al*: Methylation of the PTEN promoter defines low-grade gliomas and secondary glioblastoma. Neuro Oncol 9: 271-279, 2007.
32. Tamguney T and Stokoe D: New insights into PTEN. J Cell Sci 120: 4071-4079, 2007.
33. Wang L, Wang WL, Zhang Y, Guo SP, Zhang J and Li QL: Epigenetic and genetic alterations of PTEN in hepatocellular carcinoma. Hepatol Res 37: 389-396, 2007.
34. Pan L, Lu J, Wang X, Han L, Zhang Y, Han S and Huang B: Histone deacetylase inhibitor trichostatin a potentiates doxorubicin-induced apoptosis by up-regulating PTEN expression. Cancer 109: 1676-1688, 2007.
35. Kondo Y: Targeting histone methyltransferase EZH2 as cancer treatment. J Biochem 156: 249-257, 2014.
36. Marino-Ramirez L, Kann MG, Shoemaker BA and Landsman D: Histone structure and nucleosome stability. Expert Rev Proteomics 2: 719-729, 2005.
37. Medrzycki M, Zhang Y, McDonald JF and Fan Y: Profiling of linker histone variants in ovarian cancer. Front Biosci (Landmrk Ed) 17: 396-406, 2012.

38. Chen ZH, Zhu M, Yang J, Liang H, He J, He S, Wang P, Kang X, McNutt MA, Yin Y and Shen WH: PTEN interacts with histone H1 and controls chromatin condensation. Cell Rep 8: 2003-2014, 2014.
39. Martin M: CUTADAPT removes adapter sequences from high-throughput sequencing reads. EMBnet J 17: 10-12, 2011.
40. Dobin A, Davis CA, Schlesinger F, Drenkow J, Zaleski C, Jha S, Batut P, Chaisson M and Gingeras TR: STAR: Ultrafast universal RNA-seq aligner. Bioinformatics 29: 15-21, 2013.
41. Li B and Dewey CN: RSEM: Accurate transcript quantification from RNA-Seq data with or without a reference genome. BMC Bioinformatics 12: 323, 2011.
42. Sun J, Nishiyama T, Shimizu K and Kadota K: TCC: An R package for comparing tag count data with robust normalization strategies. BMC Bioinformatics 14: 219, 2013.
43. Love MI, Huber W and Anders S: Moderated estimation of fold change and dispersion for RNA-seq data with DESeq2. Genome Biol 15: 550, 2014.
44. Robinson MD, McCarthy DJ and Smyth GK: edgeR: A Bioconductor package for differential expression analysis of digital gene expression data. Bioinformatics 26: 139-140, 2010.
45. Liao Y, Wang J, Jaehnig EJ, Shi Z and Zhang B: WebGestalt 2019: Gene set analysis toolkit with revamped UIs and APIs. Nucleic Acids Res 47: W199-W205, 2019.
46. Young MD, Wakefield MJ, Smyth GK and Oshlack A: Gene ontology analysis for RNA-seq: Accounting for selection bias. Genome Biol 11: R14, 2010.
47. Pettersen EF, Goddard TD, Huang CC, Couch GS, Greenblatt DM, Meng EC and Ferrin TE: UCSF Chimera-a visualization system for exploratory research and analysis. J Comput Chem 25: 1605-1612, 2004.
48. Boosani CS and Agrawal DK: PTEN modulators: A patent review. Expert Opin Ther Pat 23: 569-580, 2013.
49. Zhu AX, Rosmorduc O, Evans TR, Ross PJ, Santoro A, Carrilho FJ, Bruix J, Qin S, Thuluvath PJ, Llovet JM, *et al*: SEARCH: A phase III, randomized, double-blind, placebo-controlled trial of sorafenib plus erlotinib in patients with advanced hepatocellular carcinoma. J Clin Oncol 33: 559-566, 2015.
50. Byron SA, Van Keuren-Jensen KR, Engelthaler DM, Carpten JD and Craig DW: Translating RNA sequencing into clinical diagnostics: opportunities and challenges. Nat Rev Genet 17: 257-271, 2016.
51. Garber ME, Troyanskaya OG, Schluens K, Petersen S, Thaesler Z, Pacyna-Gengelbach M, van de Rijn M, Rosen GD, Perou CM, Whyte RI, *et al*: Diversity of gene expression in adenocarcinoma of the lung. Proc Natl Acad Sci USA 98: 13784-13789, 2001.
52. Cajigas-Du Ross CK, Martinez SR, Woods-Burnham L, Durán AM, Roy S, Basu A, Ramirez JA, Ortiz-Hernández GL, Ríos-Colón L, Chirshev E, *et al*: RNA sequencing reveals upregulation of a transcriptomic program associated with stemness in metastatic prostate cancer cells selected for taxane resistance. Oncotarget 9: 30363-30384, 2018.
53. Sos ML, Koker M, Weir BA, Heynck S, Rabinovsky R, Zander T, Seeger JM, Weiss J, Fischer F, Frommolt P, *et al*: PTEN loss contributes to erlotinib resistance in EGFR-mutant lung cancer by activation of Akt and EGFR. Cancer Res 69: 3256-3261, 2009.
54. Martire S and Banaszynski LA: The roles of histone variants in fine-tuning chromatin organization and function. Nat Rev Mol Cell Biol 21: 522-541, 2020.
55. Malik HS and Henikoff S: Phylogenomics of the nucleosome. Nat Struct Biol 10: 882-891, 2003.
56. Thatcher TH and Gorovsky MA: Phylogenetic analysis of the core histones H2A, H2B, H3, and H4. Nucleic Acids Res 22: 174-179, 1994.
57. Freeman L, Kurumizaka H and Wolffe AP: Functional domains for assembly of histones H3 and H4 into the chromatin of Xenopus embryos. Proc Natl Acad Sci USA 93: 12780-12785, 1996.
58. Liu Z, Zhu Y, Gao J, Yu F, Dong A and Shen WH: Molecular and reverse genetic characterization of NUCLEOSOME ASSEMBLY PROTEIN1 (NAP1) genes unravels their function in transcription and nucleotide excision repair in Arabidopsis thaliana. Plant J 59: 27-38, 2009.
59. Ong J, van den Berg A, Faiz A, Boudewijn IM, Timens W, Vermeulen CJ, Oliver BG, Kok K, Terpstra MM, van den Berge M, *et al*: Current smoking is associated with decreased expression of miR-335-5p in parenchymal lung fibroblasts. Int J Mol Sci 20: 5176, 2019.
60. Li LM, Liu ZX and Cheng QY: Exosome plays an important role in the development of hepatocellular carcinoma. Pathol Res Pract 215: 152468, 2019.
61. Xiao Y, Zheng S, Duan N, Li X and Wen J: MicroRNA-26b-5p alleviates cerebral ischemia-reperfusion injury in rats via inhibiting the N-myc/PTEN axis by downregulating KLF10 expression. Hum Exp Toxicol 40: 1250-1262, 2021.
62. Wang Y, Sun B, Sun H, Zhao X, Wang X, Zhao N, Zhang Y, Li Y, Gu Q, Liu F, *et al*: Regulation of proliferation, angiogenesis and apoptosis in hepatocellular carcinoma by miR-26b-5p. Tumour Biol 37: 10965-10979, 2016.
63. Fan X, Kraynak J, Knisely JPS, Formenti SC and Shen WH: PTEN as a guardian of the genome: Pathways and targets. Cold Spring Harb Perspect Med 10: a036194, 2020.
64. Chew A, Salama P, Robbshaw A, Klopcic B, Zeps N, Platell C and Lawrance IC: SPARC, FOXP3, CD8 and CD45 correlation with disease recurrence and long-term disease-free survival in colorectal cancer. PLoS One 6: e22047, 2011.
65. Hafsi S, Pezzino FM, Candido S, Ligresti G, Spandidos DA, Soua Z, McCubrey JA, Travali S and Libra M: Gene alterations in the PI3K/PTEN/AKT pathway as a mechanism of drug-resistance (review). Int J Oncol 40: 639-644, 2012.